

Foreign Object Detection in Wireless Power Transfer Systems

Jianghua Lu , *Student Member, IEEE*, Guorong Zhu , *Senior Member, IEEE*,
and Chunting Chris Mi , *Fellow, IEEE*

Abstract—The successful commercialization of wireless power transfer (WPT) technology in mobile phones, laptops, and electric vehicles requires a safe, reliable, and efficient charging infrastructure. A metal object, such as a coin, a key, or a nail, however, may be inadvertently exposed, by close proximity, to the magnetic fields generated by the WPT coupler, creating a potential safety hazard and affecting the electrical characteristics of the WPT system. In addition, the magnetic fields may produce adverse symptoms, such as dizziness and breathlessness, in living objects near the charging systems. This article provides a current state of the art review of all available designs for detecting metal and living objects in WPT systems. Working principles and qualitative comparisons in terms of sensitivity, accuracy, and cost of major detection methods are presented to reveal their inherent limitations and available applications. Finally, a number of research topics on foreign object detection are suggested to encourage more researchers to make contributions to the development and commercial application of wireless charging systems.

Index Terms—Foreign object detection, living object protection, metal object detection, wireless power transfer.

I. INTRODUCTION

RECENT developments in wireless power transfer (WPT) technology [1]–[3] mean that the technology has gained wide acceptance in a range of applications, including electronic devices [4], [5], implantable electronics [6]–[8], automatic guided vehicles [9]–[11], and electric vehicles (EVs) [12]–[18]. WPT technology has some outstanding advantages compared with conventional plug-in chargers; for example, with these systems, charging can be performed automatically and without user

intervention or manipulations, thereby significantly improving the user experience. These systems also include no exposed electrical and mechanical contacts, which improves the safety and reliability of the charging infrastructure.

However, when one or more metallic foreign objects, such as coins, keys, paper clips, nuts, or bolts, are present on the transmitter (Tx) coil in a WPT system, they will dramatically affect the distribution of the magnetic fields between the Tx and receiver (Rx) coils [19], [20]. Consequently, some electrical characteristics of the WPT system, including the system transfer efficiency, output power, and quality factors of the Tx and Rx coils, inevitably change. Further, metallic foreign objects provide a path upon which eddy currents and hysteresis losses can be generated. This can cause the temperature of these objects to rise significantly [21]–[23], which may melt the plastic surface of the Tx coil. This is not an uncommon issue, either, as any users may inadvertently put their keys next to a wireless charging device that is charging a mobile phone or laptop computer. The generated eddy currents and hysteresis losses might also heat the keys and cause injuries to the user who picks up the keys. In addition to the issues regarding the metal objects, some physical symptoms, such as dizziness, breathlessness, and blood pressure change may occur in living foreign objects, such as cats, dogs, birds, and humans, that are exposed to the magnetic field generated by the WPT coupler [24]. Thus, to ensure the safety and reliability of WPT systems, it is mandatory that special precautions and designs are adopted to 1) prevent foreign objects (including conducting materials like metallic and magnetic objects and living objects) from being exposed to the charging system, 2) detect the inadvertent presence of foreign objects, and 3) take corresponding measures, such as sounding an audible alarm, actuating a visual alarm, or halting power provision to the load.

The method of designing a movable shield surrounding the WPT coupler, as shown in Fig. 1, is an effective solution to prevent foreign objects from being exposed to the charging area. However, the high cost and difficulty in installation are the drawbacks of this method and limit its application. Past research efforts on metal object detection (MOD) and living object detection (LOD, can also be referred to as living object protection) in WPT systems can be categorized as shown in Fig. 2. There is no doubt that both metal and living objects that present in the charging area cause the variation of some physical properties in the area. This means that physical sensors, such

Manuscript received July 29, 2020; revised November 23, 2020; accepted January 7, 2021. Date of publication February 5, 2021; date of current version January 19, 2022. Paper 2020-ATWPT-1260.R1, approved for publication in the IEEE TRANSACTIONS ON INDUSTRY APPLICATIONS by the Advanced and Emerging Technologies of High-efficiency and Long-distance Wireless Power Transfer Systems. This work was supported in part by the Scholarship from the China Scholarship Council and in part by the National Natural Science Foundation of China under Grants 51777146 and 51977163. (*Corresponding author: Chunting Chris Mi.*)

Jianghua Lu is with the School of Information Science and Engineering, Wuhan University of Science and Technology, Wuhan 430081, China (e-mail: jianghualu@wust.edu.cn).

Guorong Zhu is with the School of Automation, Wuhan University of Technology, Wuhan 430070, China (e-mail: zhgr_55@whut.edu.cn).

Chunting Chris Mi is with the Department of Electrical and Computer Engineering, San Diego State University, San Diego, CA 92182 USA (e-mail: cmi@sdsu.edu).

Color versions of one or more figures in this article are available at <https://doi.org/10.1109/TIA.2021.3057603>.

Digital Object Identifier 10.1109/TIA.2021.3057603

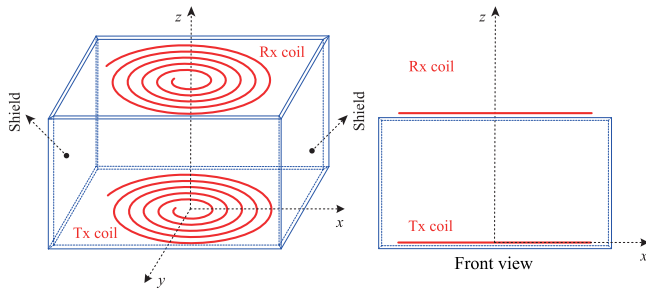


Fig. 1. A movable shield surrounding the WPT coupler.

as temperature sensors, infrared cameras, pressure sensors, and radar sensors, can be configured to detect foreign objects [25]–[32], [35]–[39]. In addition, as described above, metal objects affect the magnetic fields between the Tx and Rx coils and thus the electric characteristics of the WPT system [19]–[21], [40]–[67]. These characteristics may include the self-inductances and quality factors of the Tx and Rx coils, currents on the Tx and Rx coils, coupling coefficient, input/output powers, and efficiency. These variations of electric characteristic can also be used to indicate the presence of metal objects. Furthermore, the sensing pattern-based method [23], [32]–[34], [68]–[92] is alternatively an effective solution for detecting metal objects. This method measures variations in induced voltage or impedance of a detection coil set mounted on the Tx coil. For LOD, in addition to the sensor-based methods, the capacitive detection method, in which capacitance variation is detected, is another alternative solution [24], [35], [70], [93]. Even though some MOD and LOD methods have been proposed for a variety of applications and Zhang *et al.* [22] have reviewed the widely used FOD methods, it is still worth a comprehensive analysis of the working principle of the widely used FOD methods, because it can illustrate the essential effect of the foreign object on the WPT systems and can provide more possible detection methods. And there is a lack of quantitative analysis and comparisons of all alternative detection methods in terms of their accuracy, sensitivity, and cost, which can reveal their inherent limitations in applications. In addition, which method is the most promising solution is an open question for either/both MOD or/and LOD.

In order to gain a thorough knowledge of both MOD and LOD, this article qualitatively analyzes the influence of foreign objects on all electrical and nonelectrical characteristics of WPT systems. In theory, all variation in measurable parameters can be used to detect the presence of foreign objects. Based on the analysis, the latest achievements in FOD research are reviewed, categorized, and compared. Moreover, the limitations inherent in the available applications of major detection methods are presented. A number of suggested FOD research topics are put forward, all sharing the aim of promoting its accuracy, sensitivity, and cost-effectiveness. More specifically, Section II analyzes the working principles, features, limitations, and available applications of three different MOD methods, i.e., sensor-based detection method, system parameter detection method, and sensing pattern-based detection method. The LOD

technology is given in Section III, followed by the conclusion in Section IV.

II. METAL OBJECT DETECTION

A. Sensor-Based Detection Method

According to Faraday's law of induction, when a metallic foreign object is placed in close proximity to a time-varying magnetic field, eddy currents will be generated in the metal object, inevitably causing its temperature to rise. In addition, hysteresis losses may be generated in some metal objects as well which will further increase the temperature of the metal objects. Table I presents our experiment results of a number of metal objects present in a 3.3-kW WPT system. The results show that temperatures of all metallic objects have increased dramatically in just 2 min, especially that of the screw, which increase to approximately 102.1°C. Thermal cameras (e.g., infrared sensors) [25]–[29], temperature sensors [27], and thermistors [28] are able to sense temperature rise and provide temperature-related information to their controller to indicate the presence of metallic foreign objects.

In addition, metal objects falling on the Tx coil inevitably cause its surface to deform, which means that pressure sensors [27] can detect their presence. Besides these, radar sensors [28], [30] and image cameras [28], [31] can also be applied to identify the presence of metal objects by measuring the distance-related information between the radar transmission and reception signals and providing visual detection, respectively.

Some of these sensors, such as infrared and radar sensors as well as image cameras, can be mounted not only on the Tx side, but also on the Rx side [27], [28], [30]. On the Rx side, relatively fewer sensors are needed to protect the whole charging area, as there is a clear view of the whole charging area. Sensors mounted on the Rx side are also protected from the risk of vandalism or weather-inflicted damage.

Overall, the sensor-based method has the following advantages: 1) it is not limited by the WPT operating frequency and power level, especially in high power applications like EVs, electric bikes, etc; 2) it operates independent of misalignment between the Tx and Rx coils; 3) it can detect any metallic foreign objects; and 4) it has high sensitivity to small metal objects. However, this type of method is not free of issues. It is still the case that some nonconductive materials (e.g., wood, glass and plastic), which will not create a potential safety hazard and influence the electrical characteristics of the WPT system, may affect the detection accuracy. For example, it is difficult for a temperature sensor to detect a nail embedded in wood, and a piece of glass debris can falsely trigger a pressure or radar sensor. Additionally, some metal objects, for example, the coin and the key, exhibit insignificant temperature rise in low-power WPT systems operating at 6.78 MHz and higher frequencies [67]. It means that the temperature sensor is not suitable for detecting metal objects in these applications. Further, the relatively high cost and difficulty in installation limit the potential application of the sensor-based detection method [23], [68], especially in wireless mobile phone and laptop computer charging systems.

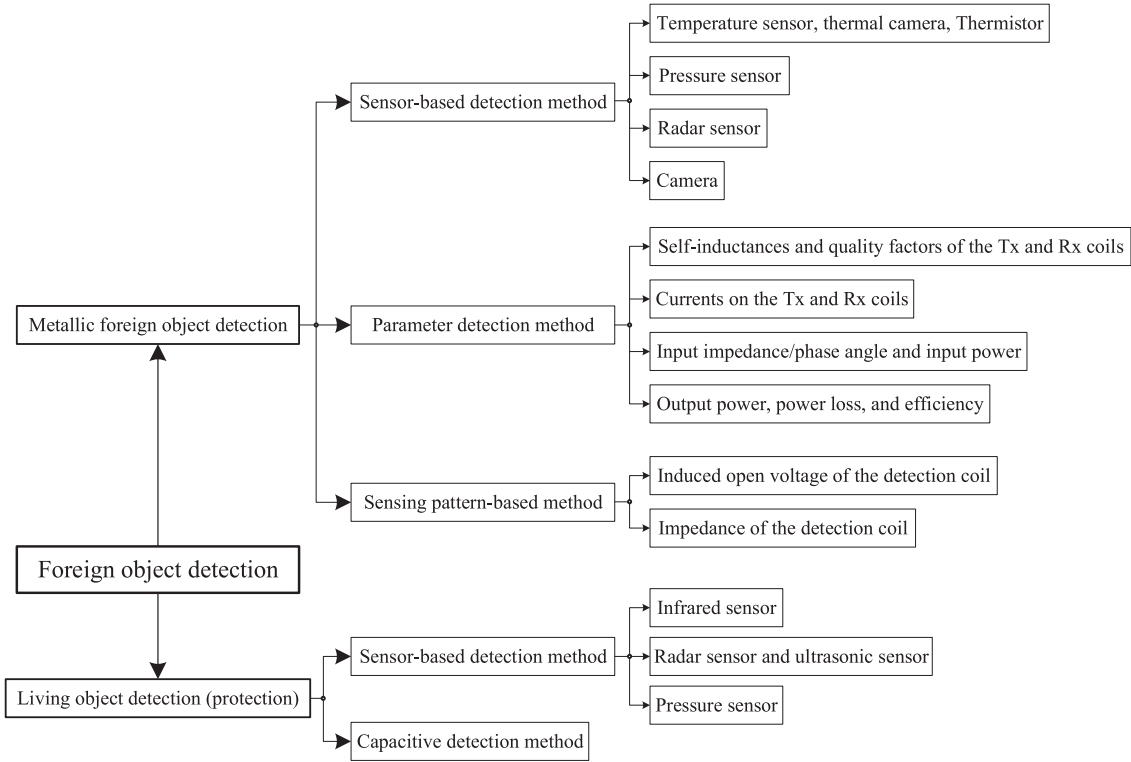


Fig. 2. Categorization of foreign object detection (FOD) in WPT systems.

TABLE I
TEMPERATURE RISE OF METAL OBJECTS PRESENT IN A 3.3-kW WPT SYSTEM AFTER 2 MIN

Metal objects	Key	US one-cent coin	US quarter dollar coin	Screw	Nail	Spring washer
Temperature rise (°C)	52.3	46.5	61.7	102.1	89.2	95.3

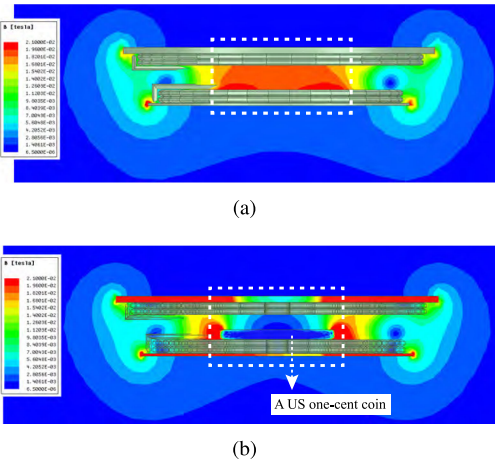


Fig. 3. Magnetic flux of a 15-W WPT system (a) without and (b) with the presence of a US one-cent coin.

B. System Parameter Detection Method

Fig. 3(a) and (b) shows the magnetic fluxes of a 15-W WPT system based on the Qi standard [94], without and with the presence of a US one-cent coin (diameter = 19.05 mm; thickness

= 1.55 mm) on the Tx coil, respectively. From Fig. 3(b), it can be seen that the coin dramatically distorts the distribution of the magnetic fluxes between the Tx and Rx coils, which consequently changes the electrical characteristics of the magnetic couplers. These variations in electrical parameters can then be used to detect the presence of metal objects. We will next present generic circuit models of a WPT system without and with the presence of a metal object and comprehensively analyze the effect of the metal object on the WPT system parameters. Based on the mathematical models of the parameters, a quantitative analysis of a US one-cent coin in two WPT systems with different power levels is presented to show the limitations and available applications of this type of method.

Fig. 4(a) shows the equivalent circuit of a series-series (SS)-compensated WPT system [1], [12], [95]. The self-inductances of the WPT coupler are represented by L_{Tx} for the transmitter and L_{Rx} for receiver. M_{TR} is the mutual inductance between the Tx and Rx coils. R_{Tx} and R_{Rx} denote the resistances of the Tx and Rx coils, respectively. C_{Tx} and C_{Rx} are the compensation capacitances on the Tx and Rx sides. V_{AB} and I_{Tx} are the phasor forms of the input voltage and current of the WPT coupler, and V_{ab} and I_{Rx} are the output variables. R_{ab} is the equivalent ac load resistance.

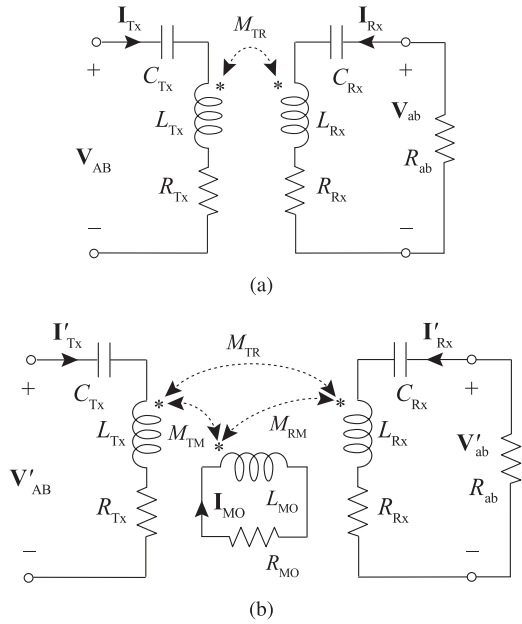


Fig. 4. Equivalent circuits of an SS-compensated WPT system (a) without and (b) with a metal object placed on the charging area.

According to the Kirchhoff's Voltage Law (KVL), the SS-compensated WPT system can be described as

$$\mathbf{V}_{AB} = \left(j\omega L_{Tx} + \frac{1}{j\omega C_{Tx}} + R_{Tx} \right) \cdot \mathbf{I}_{Tx} + j\omega M_{TR} \cdot \mathbf{I}_{Rx} \quad (1a)$$

$$\mathbf{V}_{ab} = j\omega M_{TR} \cdot \mathbf{I}_{Tx} + \left(j\omega L_{Rx} + \frac{1}{j\omega C_{Rx}} + R_{Rx} \right) \cdot \mathbf{I}_{Rx}. \quad (1b)$$

Here, $\omega (= 2\pi f)$ represents the resonant angular frequency of the WPT system and is usually set to be

$$\omega^2 = \frac{1}{L_{Tx}C_{Tx}} = \frac{1}{L_{Rx}C_{Rx}}. \quad (2)$$

By substituting (2) into (1), the system can be simplified to

$$\mathbf{V}_{AB} = R_{Tx} \cdot \mathbf{I}_{Tx} + j\omega M_{TR} \cdot \mathbf{I}_{Rx} \quad (3a)$$

$$\mathbf{V}_{ab} = j\omega M_{TR} \cdot \mathbf{I}_{Tx} + R_{Rx} \cdot \mathbf{I}_{Rx}. \quad (3b)$$

According to (3), the currents on the Tx and Rx coils (\mathbf{I}_{Tx} and \mathbf{I}_{Rx}), input impedance (Z_{in}), quality factors of the Tx and Rx coils (Q_{Tx} and Q_{Rx}), output power, and transfer efficiency are expressed as, respectively,

$$\mathbf{I}_{Tx} = \frac{(R_{Rx} + R_{ab})}{R_{Tx}(R_{Rx} + R_{ab}) + (\omega M_{TR})^2} \mathbf{V}_{AB} \quad (4)$$

$$\mathbf{I}_{Rx} = \frac{-j\omega M_{TR}}{R_{Tx}(R_{Rx} + R_{ab}) + (\omega M_{TR})^2} \mathbf{V}_{AB} \quad (5)$$

$$Z_{in} = R_{in} + jX_{in} = R_{Tx} + \frac{(\omega M_{TR})^2}{R_{ab} + R_{Rx}} \quad (6)$$

$$Q_{Tx} = \frac{1}{R_{Tx}} \sqrt{\frac{L_{Tx}}{C_{Tx}}} \quad \text{and} \quad Q_{Rx} = \frac{1}{R_{Rx}} \sqrt{\frac{L_{Rx}}{C_{Rx}}} \quad (7)$$

$$P_{out} = I_{Rx}^2 R_{ab} = \frac{(\omega M_{TR})^2 V_{AB}^2 R_{ab}}{\left(R_{Tx}(R_{Rx} + R_{ab}) + (\omega M_{TR})^2 \right)^2} \quad (8)$$

$$\begin{aligned} \eta &= \frac{P_{out}}{P_{out} + P_{loss}} = \frac{I_{Rx}^2 R_{ab}}{I_{Tx}^2 R_{Tx} + I_{Rx}^2 (R_{Rx} + R_{ab})} \\ &= \frac{\omega^2 M_{TR}^2}{R_{Rx} R_{ac} + R_{Rx}^2 + \omega^2 M_{TR}^2} \frac{R_L}{R_{Rx} + R_L}. \end{aligned} \quad (9)$$

When an MO is placed in the charging area, it will be coupled with both the Tx and Rx coils. The system equivalent circuit, in a case such as this, is shown in Fig. 4(b). In this figure, the metal object is modeled as an inductance, L_{MO} , with a series resistance, R_{MO} [22], [40], [68], [76]. The mutual inductance between the Tx coil and metal object is defined as M_{TM} , while M_{RM} represents the mutual inductance between the Rx coil and the metal object.

Also, by applying KVL to Fig. 4(b), the following equations can be obtained:

$$\begin{aligned} \mathbf{V}'_{AB} &= \left(j\omega L_{Tx} + \frac{1}{j\omega C_{Tx}} + R_{Tx} \right) \cdot \mathbf{I}'_{Tx} + j\omega M_{TR} \cdot \mathbf{I}'_{Rx} \\ &\quad + j\omega M_{TM} \cdot \mathbf{I}_{MO} \end{aligned} \quad (10a)$$

$$\begin{aligned} \mathbf{V}'_{ab} &= j\omega M_{TR} \cdot \mathbf{I}'_{Tx} + \left(j\omega L_{Rx} + \frac{1}{j\omega C_{Rx}} + R_{Rx} \right) \cdot \mathbf{I}'_{Rx} \\ &\quad + j\omega M_{RM} \cdot \mathbf{I}_{MO} \end{aligned} \quad (10b)$$

$$\begin{aligned} 0 &= j\omega M_{TR} \cdot \mathbf{I}'_{Tx} + j\omega M_{TM} \cdot \mathbf{I}'_{Rx} \\ &\quad + (j\omega L_{MO} + R_{MO}) \cdot \mathbf{I}_{MO}. \end{aligned} \quad (10c)$$

Here, \mathbf{V}'_{AB} and \mathbf{I}'_{Tx} are the phasor forms of the input voltage and current when an MO is placed in the charging area, and \mathbf{V}'_{ab} and \mathbf{I}'_{Rx} are the corresponding output variables. \mathbf{I}_{MO} represents the eddy current on the metal object. Under the resonant condition of (2), (10) can be simplified to

$$\begin{aligned} \mathbf{V}'_{AB} &= \left(R_{Tx} + \frac{(\omega M_{TM})^2}{R_{MO} + j\omega L_{MO}} \right) \cdot \mathbf{I}'_{Tx} \\ &\quad + \left(j\omega M_{TR} + \frac{\omega^2 M_{TM} M_{RM}}{R_{MO} + j\omega L_{MO}} \right) \cdot \mathbf{I}'_{Rx} \end{aligned} \quad (11a)$$

$$\begin{aligned} \mathbf{V}'_{ab} &= \left(j\omega M_{TR} + \frac{\omega^2 M_{TM} M_{RM}}{R_{MO} + j\omega L_{MO}} \right) \cdot \mathbf{I}'_{Tx} \\ &\quad + \left(R_{Rx} + \frac{(\omega M_{RM})^2}{R_{MO} + j\omega L_{MO}} \right) \cdot \mathbf{I}'_{Rx}. \end{aligned} \quad (11b)$$

And one can then obtain

$$\mathbf{I}'_{Tx} = -\frac{(j\omega L_{MO} + R_{MO})C}{B^2 - AC} \mathbf{V}'_{AB} \quad (12a)$$

$$\mathbf{I}'_{Rx} = \frac{(j\omega L_{MO} + R_{MO})B}{B^2 - AC} \mathbf{V}'_{AB} \quad (12b)$$

$$\mathbf{I}_{MO} = \frac{j\omega M_{TM}C - j\omega M_{RM}B}{B^2 - AC} \mathbf{V}'_{AB} \quad (12c)$$

TABLE II
LITERATURE REVIEW OF METAL OBJECT DETECTION BASED ON VARIATION OF ELECTRICAL CHARACTERISTICS OF WPT SYSTEMS

Electrical characteristics	References
Inductances of the transmitter and/or receiver coils	[20], [41]–[48]
Currents on the transmitter and/or receiver coils	[49]–[54]
Quality factors of the transmitter and/or receiver coils	[21], [42]–[45], [51], [55]–[59]
Input impedance/phase angle	[40], [47], [51], [60]
Input power	[61]–[63]
Output power	[40], [51]
Power loss	[21], [52], [64], [65]
Efficiency	[44], [47], [51], [55], [59], [66]

where

$$\begin{aligned}
 A &= j\omega R_{Tx} L_{MO} + R_{Tx} R_{MO} + (\omega M_{TM})^2 \\
 B &= j\omega R_{MO} M_{TR} - \omega^2 L_{MO} M_{TR} + \omega^2 M_{TM} M_{RM} \\
 C &= j\omega (R_{Rx} - R_{ab}) L_{MO} + (R_{Rx} - R_{ab}) R_{MO} + (\omega M_{RM})^2.
 \end{aligned} \quad (13)$$

Further, according to (11)–(13), the input impedance, quality factors of the Tx and Rx coils, output power, and efficiency of the SS-compensated WPT system with an MO placed on the Tx coil are expressed by the following equations:

$$\begin{aligned}
 Z'_{in} = R'_{in} + jX'_{in} &= R_{Tx} + \frac{(\omega M_{TM})^2}{j\omega L_{MO} + R_{MO}} \\
 &\quad - \frac{\left(j\omega M_{TR} + \frac{\omega^2 M_{TM} M_{RM}}{j\omega L_{MO} + R_{MO}} \right)^2}{R_{ab} + R_{Rx} + \frac{(\omega M_{RM})^2}{j\omega L_{MO} + R_{MO}}}
 \end{aligned} \quad (14)$$

$$Q'_{Tx} = \frac{\left(R_{MO}^2 + (\omega L_{MO})^2 \right) \sqrt{\frac{L_{Tx} - \frac{\omega^2 L_{MO} M_{TM}^2}{R_{MO}^2 + (\omega L_{MO})^2}}{C_{Tx}}}}{R_{Tx} \left(R_{MO}^2 + (\omega L_{MO})^2 \right) + R_{MO} (\omega M_{TM})^2} \quad (15a)$$

$$Q'_{Rx} = \frac{\left(R_{MO}^2 + (\omega L_{MO})^2 \right) \sqrt{\frac{L_{Rx} - \frac{\omega^2 L_{MO} M_{RM}^2}{R_{MO}^2 + (\omega L_{MO})^2}}{C_{Rx}}}}{R_{Rx} \left(R_{MO}^2 + (\omega L_{MO})^2 \right) + R_{MO} (\omega M_{RM})^2} \quad (15b)$$

$$P'_{out} = I'^2_{Rx} R_{ab} = \frac{(j\omega L_{MO} + R_{MO})^2 B^2}{(B^2 - AC)^2} V'^2_{AB} R_{ab} \quad (16)$$

$$\begin{aligned}
 \eta' &= \frac{P'_{out}}{P'_{out} + P'_{loss}} \\
 &= \frac{I'^2_{Rx} R_{ab}}{I'^2_{Rx} (R_{ab} + R_{Rx}) + I'^2_{MO} R_{MO} + I'^2_{Tx} R_{Tx}}.
 \end{aligned} \quad (17)$$

As can be seen from the above analysis, the MO placed in the power transfer area of a WPT system has an influence on

all of its electrical parameters, i.e., the self-inductances and quality factors of the Tx and Rx coils, currents on the Tx and Rx coils, input impedance (magnitude and phase), output power, and system efficiency. Therefore, variations in one or more of these electrical characteristics can be used to detect the presence of metal objects. Table II summarizes some of the published literature in which the presence of metallic foreign objects was determined based on the variation of the WPT system's electrical characteristics. Here, it should be pointed out that the Qi standard [21] for low-power WPT applications, and the WPT system parameters variation, e.g., power loss and coupling factor, are applied to detect the metal objects.

Although this type of detection method is simple, has a low cost, and requires no additional installation space, its application is limited by the WPT system power level. Furthermore, the detection accuracy of this type of method can be compromised by misalignment between the Tx and Rx coils, as well as by the equivalent resistance of the battery pack. Next, we will quantitatively analyze the effect of a US one-cent coin on the electrical characteristics of two WPT systems with different power levels to reveal the inherent limitations of this type of method in detail.

Fig. 5(a) shows a 15-W WPT coupler with an air gap of 5 mm. The geometry of the Tx and Rx coils is in compliance with the Qi standard [94]. When a US one-cent coin was placed on the Tx coil, the variations (%) of the self-inductances of the Tx and Rx coils and coupling coefficient are measured, and these are shown in Fig. 6(a). It can be seen that the presence of the coin on the Tx coil dramatically affected L_{Tx} , L_{Rx} , and k . For example, the variation of the self-inductance of the Tx coil (ΔL_{Tx}) is up to 23.2% when the coin was placed on the center of the Tx coil. Then, according to (12) and (14)–(17), the variation of L_{Tx} , L_{Rx} , or k leads to changes in the currents on the Tx and Rx coils, input impedance (magnitude and phase), quality factors of the Tx and Rx coils, output power, and efficiency of the system. This means that the coin significantly affects some of system's electrical characteristics and that the parameter detection method may be an effective solution for detecting metal objects in low-power WPT systems like mobile phones, tablets, etc.

Fig. 5(b) shows a 3.3-kW wireless EV charging system based on the SAE J2954 standard [99]. The effect of a coin on this system is shown in Fig. 6(b). According to the results, the coin

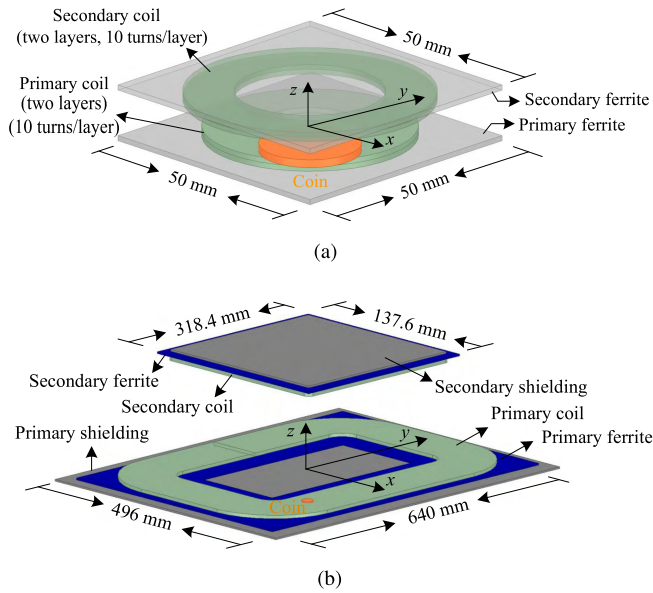


Fig. 5. (a) A 15-W WPT coupler based on the Qi standard [94] and (b) a 3.3-kW wireless EV charging coupler based on the SAE J2954 standard [99].

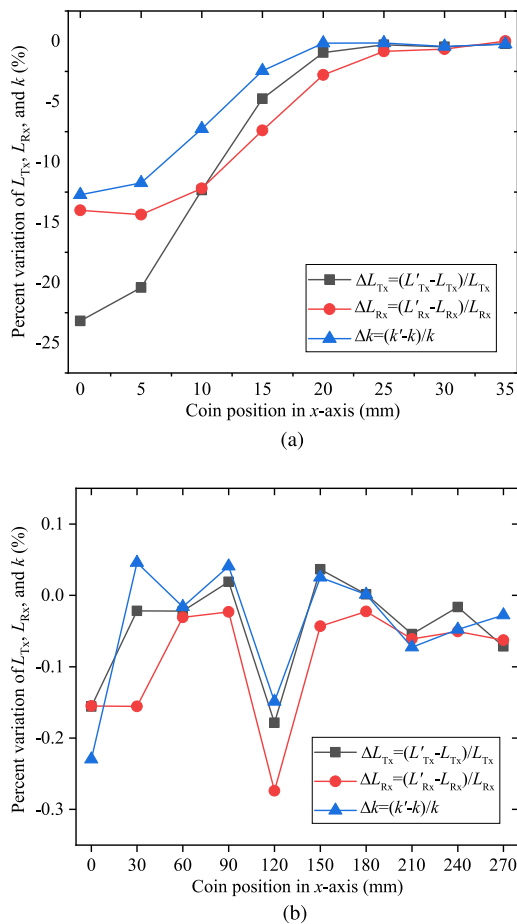


Fig. 6. Effect of a US one-cent coin on L_{Tx} , L_{Rx} , and k in (a) the 15-W WPT system and (b) the 3.3-kW WPT system. The horizontal axis origin represents the coin being placed on the center of the Tx coil.

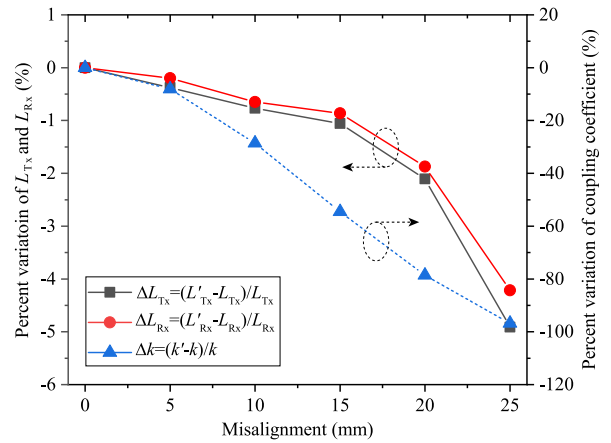


Fig. 7. Self-inductances and coupling coefficient variations with respect to misalignment in the 15-W WPT system.

caused only a negligible disturbance to the system parameters. This indicates that detection by monitoring the variation of electrical characteristics may be difficult for high power (high air-gap between the Tx and Rx coils) systems [23].

Additionally, misalignment in the lateral and/or longitudinal directions and air gap variation between the Tx and Rx coils are inevitable and these will also affect the electrical characteristics of the WPT systems [68], [100]–[102]. Fig. 7 shows the variations of the self-inductances and coupling coefficient with respect to the misalignment in the 15-W WPT system. It can be observed that the coupling coefficient decreased by about 80% when there was a 20-mm horizontal misalignment between the Tx and Rx coils. Furthermore, the output current and voltage, output power, and efficiency of the WPT system usually vary with the battery charging process [97], [98], [103], [104], and are affected by the condition of the battery, such as state of charge (SOC), temperature, and aging. Therefore, it is a challenge to distinguish the system parameter variation caused by the presence of metal objects, potential misalignment between the Tx and Rx coils, or different battery state.

C. Sensing Pattern-Based Detection Method

The sensing pattern-based detection method has also proved to be a viable alternative for the detection of metallic foreign objects in WPT systems, especially in high power applications. In this method, one or more detection coils [69]–[73], as shown in Fig. 8, are mounted onto the WPT coupler. Fig. 9 shows an example of a WPT coupler with a number of detection coils. The variation of the electrical characteristic of the detection coil, such as its induced open-circuit voltage or impedance variation, is then sensed to indicate the presence of the metal objects.

1) *Induced Voltage Detection*: Fig. 10(a) shows the equivalent circuit of a WPT system with a detection coil mounted on the Tx coil. L_D and R_D represent the self-inductance and parasitic resistance of the detection coil, respectively. M_{TD} and M_{RD} are the mutual inductances between the detection coil and the Tx coil and Rx coil. The open-circuit voltage (V_D) of the detection

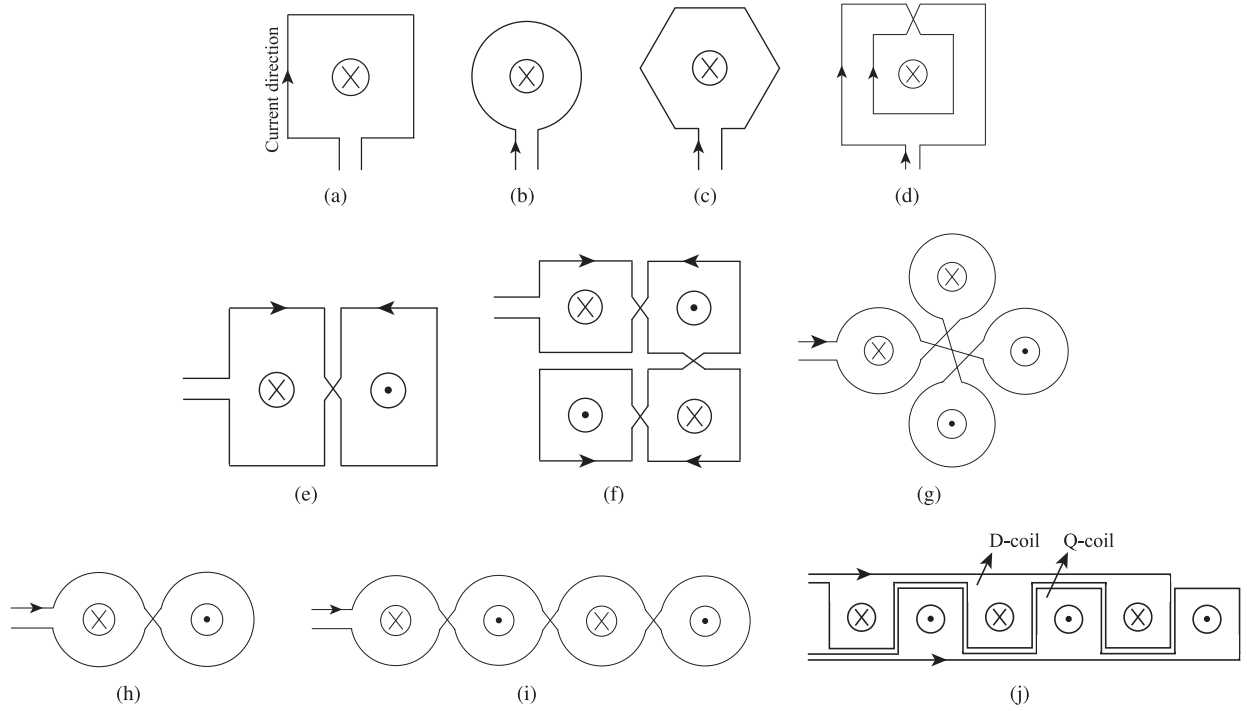


Fig. 8. Different types of detection coils. (a) Rectangular (or square) coil, (b) circular coil, (c) hexagonal coil [71], (d) rectangular double loop coil [71], (e) double-D coil [71], (f) quadruple-D coil [71], (g) four-lobe configuration of aligned magnetic quadrupoles [70], (h) two-lobe configuration of two conductor loops arranged to have opposed magnetic dipoles [70], (i) four-lobe configuration of conductor loops extending in a linear dimension [70], and (j) nonoverlapping DQ-coil [69].

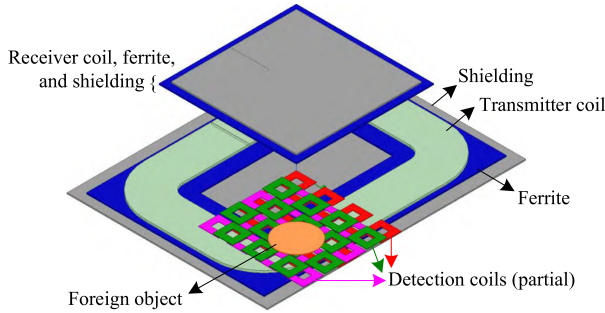


Fig. 9. A detection coil set in a WPT system.

coil induced by the time-varying magnetic field generated by the WPT coupler can be expressed as

$$V_D = j\omega M_{TD} I_{Tx} + j\omega M_{RD} I_{Rx}. \quad (18)$$

Fig. 10(b) shows the equivalent circuit of a WPT system when a metal object is placed on the detection coil. The metal object is mutually coupled with the Tx, Rx, and detection coils. The mutual inductances are represented by M_{TM} , M_{RM} , and M_{DM} , respectively. In this case, the induced open-circuit voltage of the detection coil is given by

$$V'_D = j\omega M_{TD} I'_{Tx} + j\omega M_{RD} I'_{Rx} + j\omega M_{DM} I_{MO}. \quad (19)$$

Compared with (18) and (19), the eddy current (I_{MO}) of the metal object placed in the proximity of the detection coil changes its induced voltage. The induced voltage variation can then be used to indicate the presence of the metal objects [73], [75]–[78].

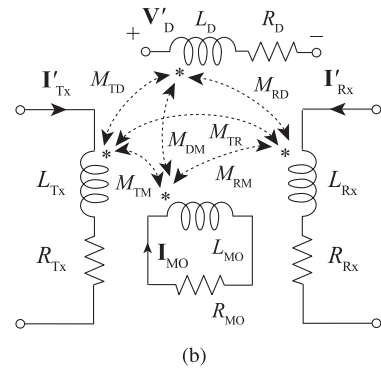
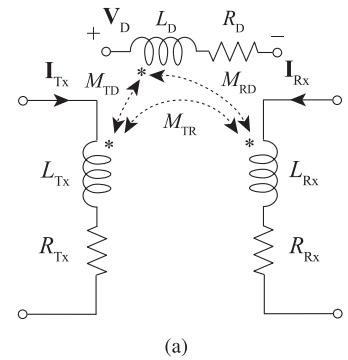


Fig. 10. Equivalent circuits of a WPT system (a) without and (b) with a metal object placed on the detection coil set.

As mentioned above, however, the currents on the Tx and Rx coils may vary with power level, which means that the detection accuracy of the method based on induced voltage variation is

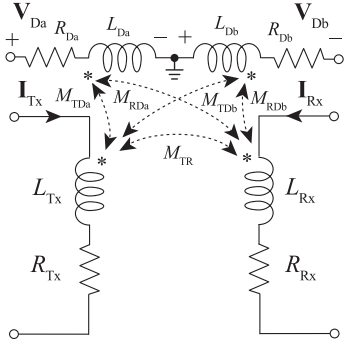


Fig. 11. An equivalent circuit of a WPT system coupling with two symmetrical detection coils.

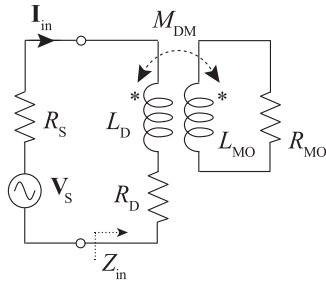
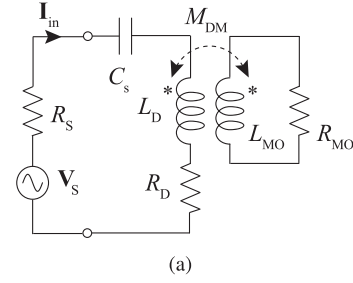


Fig. 12. Equivalent circuit of the detection coil under the influence of a metal object.

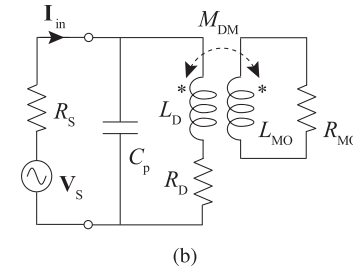
influenced by the working state of the WPT system. To address this issue, the induced voltage difference of two symmetrical detection coils can be configured to detect the presence of the metal objects [23], [69], [74]. Fig. 11 shows an equivalent circuit of a WPT system coupled with two symmetrical detection coils. The voltage induced by the magnetic field crossing the surface area of one of the coils is approximately equal and opposite to that by the magnetic field crossing the area of one of the other coils. Therefore, The induced voltage difference ($V_{Da} - V_{Db}$) of these two detection coils is substantially zero and independent of the system output power in the absence of the metal objects. If the voltage difference exceeds the predetermined threshold value, it will indicate that an MO is present on the detection coils. Additionally, the induced voltages of detection coils decoupled from the Tx coil (for example, a bipolar pad is adopted for the detection coil, while the Tx coil is an unipolar pad) can also be configured to detect metal objects [70], [79]–[81]. The working principles of these types of detection coils are similar to those of the two symmetrical coils. The induced voltage is no longer zero when metal objects present on these detection coils.

2) *Impedance Variation Detection*: Fig. 12 shows the equivalent circuit model of a detection coil under the influence of a metallic foreign object. The detection coil is excited by a sinusoidal signal source with a voltage V_s and a frequency ω_D . Usually, ω_D is designed to be different from the operating frequency of the WPT system to minimize its interaction with the WPT system and improve its sensitivity to foreign objects.

Without and with the presence of a metal object on the charging area, the input impedances of Fig. 12 can be expressed



(a)



(b)

Fig. 13. Two basic types of resonance circuits configured to amplify the impedance variation of the detection coil: (a) series and (b) parallel.

as, respectively,

$$Z_{in-w} = R_D + j\omega_D L_D \quad (20)$$

$$\begin{aligned} Z_{in-w} &= R_D + j\omega_D L_D + \frac{(\omega_D M_{DM})^2}{R_{MO} + j\omega_D L_{MO}} \\ &= \left(R_D + \frac{(\omega_D M_{DM})^2 R_{MO}}{R_{MO}^2 + (\omega_D L_{MO})^2} \right) \\ &\quad + j\omega_D \left(L_D - \frac{(\omega_D M_{DM})^2 L_{MO}}{R_{MO}^2 + (\omega_D L_{MO})^2} \right). \end{aligned} \quad (21)$$

From (20) and (21), it can be seen that both the equivalent resistance and inductance of the detection coil change with the presence of a metal object. This means that the impedance variation of the detection coil can also be used as an indicator for the presence of metallic foreign objects [32], [33], [68], [71], [82]–[90].

However, the effect of a relatively small metallic foreign object on the impedance variation of the detection coil is too small to be detected directly. For example, the self-inductance and resistance of a detection coil having a square size of 60 mm and 21 turns decreased and increased by only 3.03% and 1.83%, respectively, when a US one-cent coin was present on the center of the detection coil. To amplify and convert the impedance variation to an easily detectable voltage or frequency signal, a capacitive network is usually added to resonate with the detection coil [68], [71], [85]–[88]. In addition, the resonant network can also suppress and filter the voltage induced by the alternating electromagnetic field used for transferring power as well as the noise of harmonics. Fundamentally, there are two types of resonance topologies, series and parallel, as shown in Fig. 13(a) and (b), respectively. These were analyzed and compared in [68] and it was determined that the parallel resonance is the better

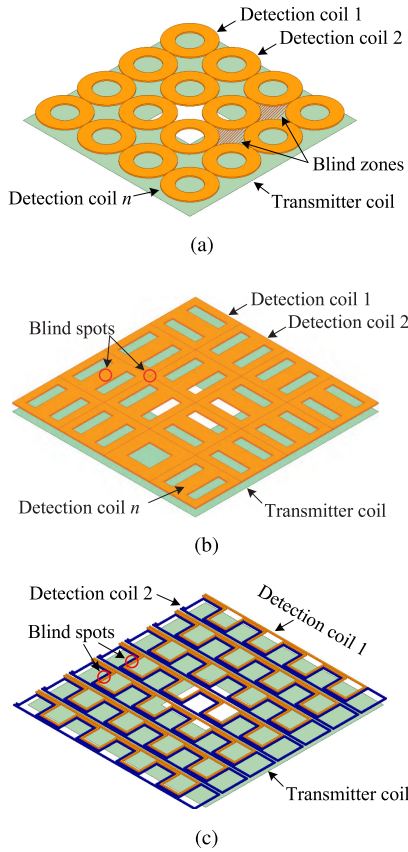


Fig. 14. Different detection coil sets [69], [72], [89].

option because of its high sensitivity to the presence of foreign objects and its high signal-to-noise ratio. In addition to the series and parallel resonances, any other type of resonant networks, such as series-parallel mixed-resonance [85], [88], can also be used to amplify the impedance variation.

3) *FOD System Design*: A metallic foreign object may fall anywhere in the charging area of a WPT system. To protect the whole charging area and improve the sensitivity to small metal objects, a plurality of detection coils configured as grid spaces in a column and row format [69], [70], [72], [73], [82], [83], [86], [89], [91], [92], such as that shown in Fig. 14(a)–(c), can be applied to detect the metal objects. For these detection coil sets, however, the blind spots/zones, where the foreign object cannot be detected because of the effect of the metal object on the induced voltage or impedance variation of the detection coil, may be substantially negligible, and this is a problem that need to be addressed. Multilayer detection coil sets deposited on each other, for example, as shown in Fig. 15(a)–(c), are an effective way of reducing or eliminating the blind spots [74], [82]. In addition, in [23], a single-layer nonoverlapping sensing coil set that will completely eliminate the problem of the blind zone is proposed, as shown in Fig. 16.

For the detection coil set shown in Fig. 16, an overall FOD system is proposed in [23], as shown in Fig. 17. In this system, the induced voltage difference of two symmetrical detection coils

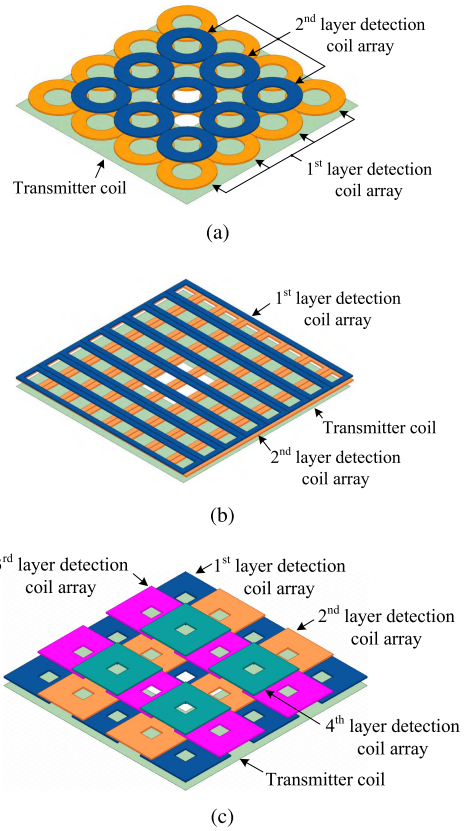


Fig. 15. Different types of multilayer detection coil set to reduce or eliminate the blind spots [74].

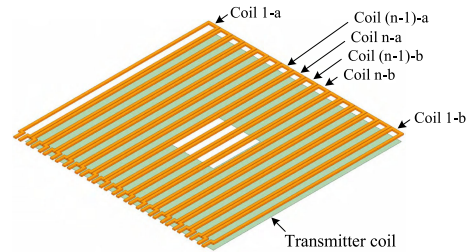


Fig. 16. A nonoverlapping symmetric sensing coil array to eliminate the blind spots [23].

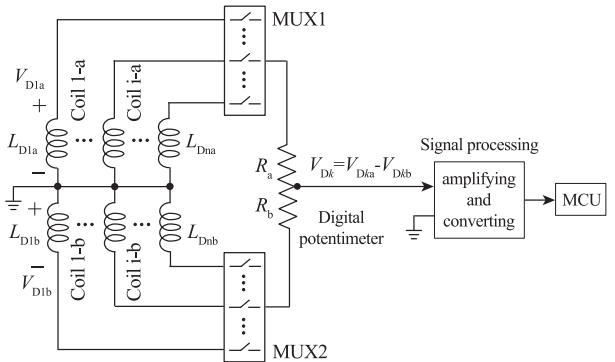


Fig. 17. A FOD system based on induced voltage variation of the detection coils [23].

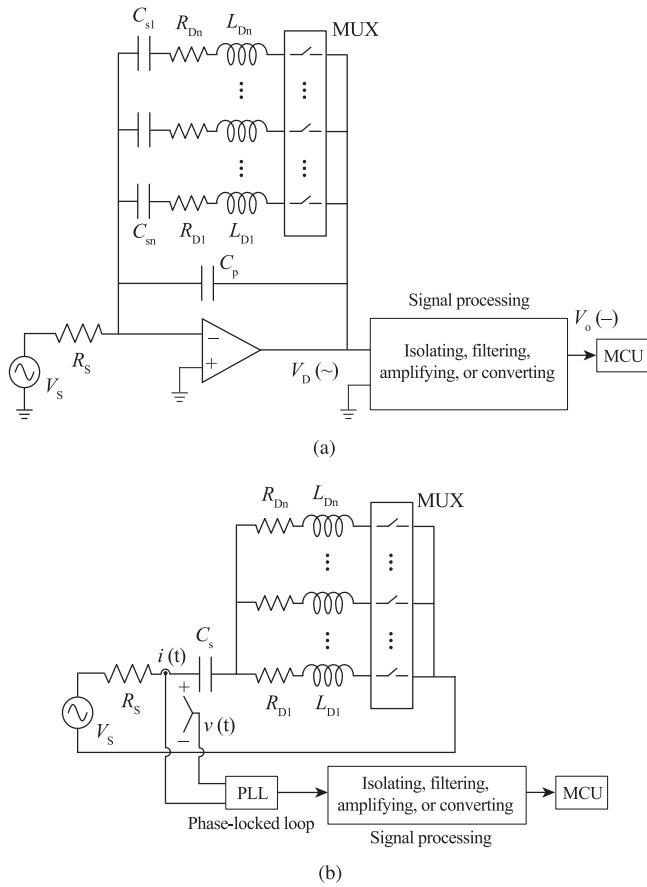


Fig. 18. Two different FOD systems based on the self-inductance variation of the detection coils. The self-inductance variation is converted to (a) a voltage signal [68] or (b) a phase signal [88].

is used to indicate the presence of metal objects. Specifically, two multiplexers (MUX) are required to make sure that only two symmetrical detection coils (for example, coil 1-a and coil 1-b) are activated at a time and to eliminate interference from other detection coils. A digital potentiometer is then used to ensure that the induced voltage difference is always zero in the absence of a metal objects, regardless of the manufacturing error and the misalignment of the Tx and Rx coils. Finally, a signal conditioning circuit is configured to improve the signal-to-noise ratio and modulate the output signal to be controlled by a microcontroller unit (MCU). The MCU stores the measured data and compares it with the reference value to indicate the presence of a metal object by sounding an audible alarm or actuating a visual alarm.

As mentioned above, in addition to sensing the induced voltage variation of the detection coil, its self-inductance variation can also be measured to detect the presence of metal objects. Fig. 18(a) and (b) shows two examples of such an FOD system [68], [88]. Similar to Fig. 17, an MUX is also adopted to control the detection coils time-divisionally in both of these systems. The capacitors are designed to resonate with the detection coil to amplify the impedance variation of the detection coil and convert it to a voltage [Fig. 18(a)] or phase signal [Fig. 18(b)] that can be easily and accurately measured.

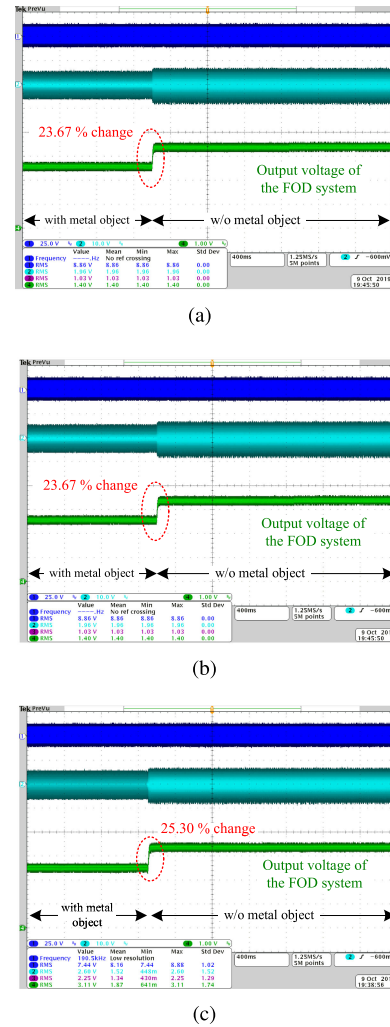


Fig. 19. Experimental results of the FOD system with the effect of different metal objects. (a) A US one-cent coin, (b) a key, and (c) a 32 × 30 mm² aluminum block. It should be pointed out that the metal objects were removed from the charging area, which can ensure that different metal objects were placed in the same position for the sake of a fair comparison.

Finally, the measured voltage or phase signal is isolated, filtered, amplified, and converted so it can be controlled by an MCU.

Although this type of method has been proven to accurately detect some metal objects [23], [68], it is necessary to conduct a comprehensive evaluation of all common metallic foreign object. Then, according to Fig. 18(a), a 3.3-kW WPT prototype with FOD function included was implemented. Some metal objects were applied to evaluate the performance of the FOD system. Fig. 19 shows the experimental results when a US one-cent coin, a key, and an aluminum block were placed on the detection coil set. It can be seen that the output voltage of the FOD system changes up to 23.67%, 28.61%, and 25.30%, respectively. The experimental results of other metal objects are shown in Table III. The results reveal that this method can detect most of the metal objects; however, a couple of the relatively small metal objects, the paper clip and staple, were not detected. Although decreasing the detection coil size would be an effective way to improve sensitivity to these small metal objects, it inevitably increases

TABLE III
EXPERIMENTAL RESULTS WITH A VARIETY OF METAL OBJECTS

Metal objects	$\frac{V_{o-w} - V_{o-w/o}}{V_{o-w/o}} \times 100\%$
US quarter dollar coin	27.30
Steel wool	26.58
Aluminum foil (20 × 20 mm ²)	34.52
Hex cap screw	5.29
Nail	4.12
Paper clip	0.61
Staple	0.43

system cost and complexity. Additionally, this method fails to detect certain small ferromagnetic objects, such as nails, screws, spring washers, and so forth.

D. Comparison and Discussion

Table IV summarizes the performance comparison of all available MOD methods according to the above analysis. Relatively speaking, the method of detecting changes in electrical characteristics of the WPT system is the simplest and most economical solution. In addition, it has the fastest detection and reaction time. Its application, however, is limited to low-power WPT systems. Furthermore, the misalignment between the Tx and Rx coils and the variation of the battery condition (such as state of charge, temperature, and aging) inevitably affect its detection accuracy. The sensor-based and sensing pattern-based methods work independent of the abovementioned misalignment and WPT power level in theory. However, high cost and difficulty in installation limit the practical application of the sensor-based method, which additionally is susceptible to some nonconductive materials and the environment. The sensor temperature may take tens of seconds or even minutes to detect the presence of metal objects. During the reaction time, the WPT system will be operating in a low-efficiency condition. For the sensing pattern-based method, designing a detection coil set to 1) make no contribution to any power loss of the WPT system, 2) cover the whole charging area and eliminate the blind spot, and 3) improve sensitivity to small metal objects and ferromagnetic objects is an additional challenge.

III. LIVING OBJECT DETECTION

There is no doubt that living objects that appear on the Tx coil will cause variations of some non-electrical characteristics of WPT systems, including the surface deformation of the Tx coil. Therefore, sensor-based detection methods, such as those using pressure sensors, infrared sensors [26], [35], radar sensors [32], [35]–[39], ultrasonic sensors [35], or image cameras, can be used to detect the presence of living objects.

The capacitive detection method [70] is another available solution for detecting the presence of living objects. In this method, the equivalent capacitance variation of the detection system is used to indicate the presence of living objects. In patent [35], multiple metal plates are mounted around the Tx coil. When living matter is not within a distance sufficient to be coupled

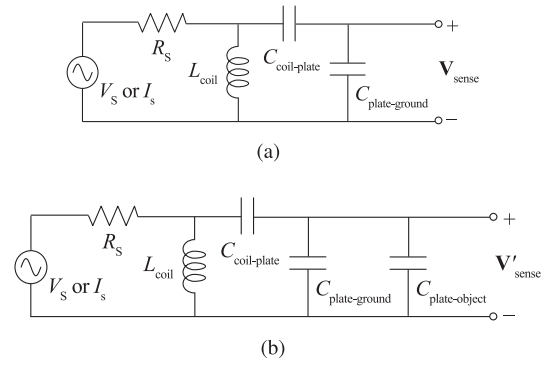


Fig. 20. Equivalent circuits of the LOD system (a) without and (b) with a living object present in the charging area [35].

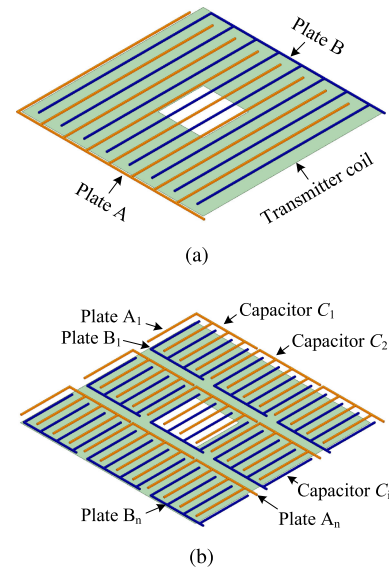


Fig. 21. (a) A comb pattern capacitor sensor [24] and (b) a multiple comb pattern capacitor sensor [93] for detecting of living objects.

with any of the metal plates, the capacitive detection system is modeled in Fig. 20(a). When a living object, for example, a dog or a cat, comes in the proximity of the charging area, an extra capacitance is added between the object and the plate, as shown in Fig. 20(b). The added capacitor will cause a change in the amplitude and/or phase of the voltage on the capacitor between the metal plate and ground ($C_{\text{plate-GND}}$), thus indicating the presence of living objects. In addition, a comb pattern capacitive sensor [24] and a multiple comb pattern capacitor sensor [93], as shown in Fig. 21(a) and (b), respectively, have been proposed to detect living objects. The presence of living objects on the charging area will cause the capacitance variation of the comb pattern capacitor sensor. Then, an inductive network is added to amplify and convert the capacitance variation to an easily detectable voltage signal. The overall detection system is shown in Fig. 22.

There is less literature on LOD than on MOD for WPT systems. Further, both the sensor-based method and the capacitive

TABLE IV
SUMMARY AND COMPARISON OF ALL MOD METHODS

MOD methods	Features	Advantages	Disadvantages
Sensor-based	* Temperature sensor, thermal camera (e.g., infrared sensors), and thermistor	* High sensitivity * Independent of WPT system power level, operating frequency and misalignment * Can detect any metal objects	* High cost * Difficult to distinguish the metal objects and non-conductive materials (stones, plastics, and glasses) * Be susceptible to the environment (temperature, dust, and rain) * Take up a large installation space
	* Pressure sensor		
	* Radar sensor		
	* Image camera		
Parameter variation	* Self-inductances of the Tx and Rx coils * Quality factors of the Tx and Rx coils * Currents on the Tx and Rx coils * Input impedance/phase angle * Input power, output power, power loss, and efficiency	* Low cost * Require no additional space * Simple * High detection speed * Appropriate for IPT and CPT systems	* Limited to low power applications * Even in low WPT system, its detection accuracy is susceptible to the misalignment and different SOC of the battery load.
Sensing pattern-based	* Induced voltage of the detection coil (or induced voltage difference) * Impedance of the detection coil	* High sensitivity * High accuracy * Not affected by non-conductive materials * Independent of the environment, and misalignment	* Detection coil set should be designed carefully to make no contribution to any power losses, eliminate the blind spots and improve the sensitivity * Cannot accurately detect small ferromagnetic objects

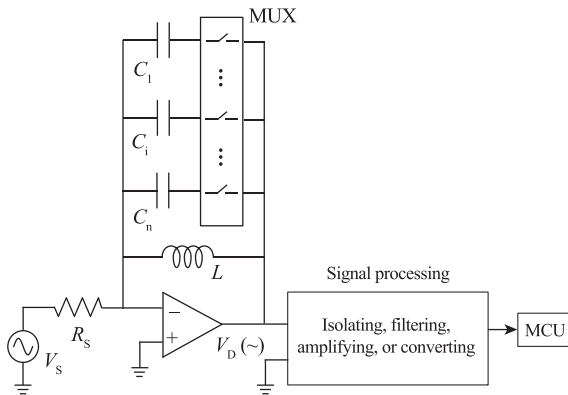


Fig. 22. A living object detection system that senses capacitances variation [93].

detection method may be difficult to use in practical applications. The sensor-based method is limited by its vulnerability to nonconductive materials and its high cost. One major issue with the capacitive detection method is that eddy current is generated in the capacitor plates, which will lead to their temperature rise and affect performances of the WPT system. In addition, the capacitive detection method typically has a low signal-to-noise ratio.

IV. CONCLUSION

This article presents the overview of MOD and LOD in WPT systems. The working principles, challenges, available applications, and comparisons of all detection methods were presented. Based on the literature review, the following conclusions and suggested research topics will be critical for the commercialization of WPT technology.

Conclusion. a) The sensor-based method can be used to detect the presence of both metal and living objects of any size and is independent of the WPT power level and misalignment between the Tx and Rx coils. However, its cost and installation space

should be taken carefully into consideration in practical applications. In addition, some nonconductive materials will affect its detection accuracy. b) Although detecting the parameter variation of the WPT system is the simplest and most economical method to sense the presence of metal objects, the application of this method is limited by the WPT system power level, misalignment between the Tx and Rx coils, and battery condition. c) The sensing pattern-based detection method has recently been the most popular solution for detecting the presence of metal objects because it has a high accuracy, is inexpensive, and easy to install. However, the detection coil set used in this method should be designed carefully to eliminate blind spots and improve sensitivity to small metal objects.

Suggested Research Topics. a) The integration of different detection methods would contribute to the sensitivity, accuracy, signal-to-noise ratio, and object localization. b) A method that can detect metal and living objects simultaneously and is not influenced by nonconductive materials and the environment is desirable. (c) MOD and LOD are necessary for capacitive power transfer systems. d) The EMI/EMC issues. e) Rather than halting the provision of power to the load, an effective approach for removing metal and living objects without user intervention should be of paramount importance.

REFERENCES

- [1] C. T. Rim and C. C. Mi, *Wireless Power Transfer for Electric Vehicles and Mobile Devices*. Hoboken, NJ, USA: Wiley-IEEE Press, 2017.
- [2] G. A. Covic and J. T. Boys, "Inductive power transfer," *Proc. IEEE*, vol. 101, no. 6, pp. 1276–1289, Jun. 2013.
- [3] S. Y. R. Hui, "Past, present and future trends of non-radiative wireless power transfer," *CPSS Trans. Power Electron. Appl.*, vol. 1, no. 1, pp. 83–91, Dec. 2016.
- [4] S. Jeong *et al.*, "Smartwatch strap wireless power transfer system with flexible PCB coil and shielding material," *IEEE Trans. Ind. Electron.*, vol. 66, no. 5, pp. 4054–4064, May 2019.
- [5] J. Park *et al.*, "A resonant reactive shielding for planar wireless power transfer system in smartphone application," *IEEE Trans. Electromagn. Compat.*, vol. 59, no. 2, pp. 695–703, Apr. 2017.
- [6] C. Liu, C. Jiang, J. Song, and K. T. Chau, "An effective sandwiched wireless power transfer system for charging implantable cardiac pacemaker," *IEEE Trans. Ind. Electron.*, vol. 66, no. 5, pp. 4108–4117, May 2019.

- [7] O. Knecht, R. Bosshard, and J. W. Kolar, "High-efficiency transcutaneous energy transfer for implantable mechanical heart support systems," *IEEE Trans. Power Electron.*, vol. 30, no. 11, pp. 6221–6236, Nov. 2015.
- [8] C. Xiao, D. Cheng, and K. Wei, "An LCC-C compensated wireless charging system for implantable cardiac pacemakers: Theory, experiment, and safety evaluation," *IEEE Trans. Power Electron.*, vol. 33, no. 6, pp. 4894–4905, Jun. 2018.
- [9] A. Zaheer, G. A. Covic, and D. Kacprzak, "A bipolar pad in a 10-kHz 300-W distributed IPT system for AGV applications," *IEEE Trans. Ind. Electron.*, vol. 61, no. 7, pp. 3288–3301, Jul. 2014.
- [10] F. Lu *et al.*, "A tightly-coupled inductive power transfer system for low-voltage and high-current charging of automatic guided vehicles," *IEEE Trans. Ind. Electron.*, vol. 66, no. 9, pp. 6867–6875, Sep. 2019.
- [11] S. Huang, T. Lee, W. Li, and R. Chen, "Modular on-road AGV wireless charging systems via interoperable power adjustment," *IEEE Trans. Ind. Electron.*, vol. 66, no. 8, pp. 5918–5928, Aug. 2019.
- [12] S. Li and C. C. Mi, "Wireless power transfer for electric vehicle applications," *IEEE Trans. Emerg. Sel. Topics Power Electron.*, vol. 3, no. 1, pp. 4–17, Mar. 2015.
- [13] D. Patil, M. K. McDonough, J. M. Miller, B. Fahimi, and P. T. Balsara, "Wireless power transfer for vehicular applications: Overview and challenges," *IEEE Trans. Transport. Electrification.*, vol. 4, no. 1, pp. 3–37, Mar. 2018.
- [14] G. A. Covic and J. T. Boys, "Modern trends in inductive power transfer for transportation applications," *IEEE Trans. Emerg. Sel. Topics Power Electron.*, vol. 1, no. 1, pp. 28–41, Mar. 2013.
- [15] C. C. Mi, G. Buja, S. Y. Choi, and C. T. Rim, "Modern advances in wireless power transfer systems for roadway powered electric vehicles," *IEEE Trans. Ind. Electron.*, vol. 63, no. 10, pp. 6533–6545, Oct. 2016.
- [16] F. Lu, H. Zhang, H. Hofmann, and C. C. Mi, "A double-sided LCLC compensated capacitive power transfer system for electric vehicle charging," *IEEE Trans. Power Electron.*, vol. 30, no. 11, pp. 6011–6014, Nov. 2015.
- [17] R. Tavakoli and Z. Pantic, "Analysis, design, and demonstration of a 25-kW dynamic wireless charging system for roadway electric vehicles," *IEEE Trans. Emerg. Sel. Topics Power Electron.*, vol. 6, no. 3, pp. 1378–1393, Sep. 2018.
- [18] Z. Cong *et al.*, "High-efficiency contactless power transfer system for electric vehicle battery charging application," *IEEE Trans. Emerg. Sel. Topics Power Electron.*, vol. 3, no. 1, pp. 65–74, Mar. 2015.
- [19] H. Jafari, M. Moghaddami and A. Sarwat, "Foreign object detection in inductive charging systems based on primary side measurements," *IEEE Trans. Ind. Appl.*, vol. 55, no. 6, pp. 6466–6475, Nov.–Dec. 2019.
- [20] M. Moghaddami and A. Sarwat, "A sensorless conductive foreign object detection for inductive electric vehicle charging systems based on resonance frequency deviation," in *Proc. IEEE Ind. Appl. Soc. Annu. Meeting*, Portland, OR, USA, 2018, pp. 1–6.
- [21] *The Qi Wireless Power Transfer System Power Class 0 Specification: Reference Designs*, Wireless Power Consortium, Feb. 2017, parts 1 and 2.
- [22] Y. Zhang, Z. Yan, J. Zhu, S. Li, and C. C. Mi, "A review of foreign object detection (FOD) for inductive power transfer systems," *eTransportation*, 2019.
- [23] V. X. Thai, G. C. Jang, S. Y. Jeong, J. H. Park, Y. Kim and C. T. Rim, "Symmetric sensing coil design for the blind-zone free metal object detection of a stationary wireless electric vehicles charger," *IEEE Trans. Power Electron.*, vol. 35, no. 4, pp. 3466–3477, Apr. 2020.
- [24] S. Y. Jeong, H. G. Kwak, G. C. Jang, and C. T. Rim, "Living object detection system based on comb pattern capacitive sensor for wireless EV chargers," in *Proc. IEEE 2nd Ann. Southern Power Electron. Conf.*, Auckland, 2016, pp. 1–6.
- [25] H. P. Widmer, "Foreign object detection using infrared sensing," U.S. Patent, 15/440516, Aug. 23, 2018.
- [26] T. Sonnenberg, A. Stevens, A. Dayerizadeh, and S. Lukic, "Combined foreign object detection and live object protection in wireless power transfer systems via real-time thermal camera analysis," in *Proc. IEEE Appl. Power Electron. Conf. Expo.*, Anaheim, CA, USA, 2019, pp. 1547–1552.
- [27] K. L. Hall, M. P. Kesler, R. Fiorello, D. A. Schatz, K. J. Kulikowski, and M. Soljacic, "Vehicle charger safety system and method," U.S. Patent, 14/087,512, Mar. 27, 2014.
- [28] A. G. Briz, A. M. Gilbert, and G. Ombach, "Methods and systems for object detection and sensing for wireless charging systems," U.S. Patent, 14/307285, Aug. 15, 2017.
- [29] A. Karanth, H. H. K. R. Dorairaj, and B. R. Kumar, "Foreign object detection in inductive coupled wireless power transfer environment using thermal sensors," U.S. Patent. 13/808786, Jun. 27, 2013.
- [30] H. Widmer, L. Sieber, A. Daetwyler, and M. Bittner, "Systems, methods, and apparatus for radar-based detection of objects in a predetermined space," U.S. Patent, 14/335296, Sep. 26, 2017.
- [31] A. Azad, V. Kulyukin, and Z. Pantic, "Misalignment tolerant DWPT charger for EV roadways with integrated foreign object detection and driver feedback system," in *Proc. IEEE Trans. Electrification. Conf. Expo.*, Detroit, MI, USA, 2019, pp. 1–5.
- [32] B. Dimke and M. Stamenic, "Wireless charging transmitter with foreign object and living object detection systems," U.S. Patent, 16/292,792, Jun. 27, 2019.
- [33] V. X. Thai, J. H. Park, S. Y. Jeong, C. T. Rim, and Y. Kim, "Equivalent-circuit-based design of symmetric sensing coil for self-inductance-based metal object detection," *IEEE Access*, vol. 8, pp. 94190–94203, 2020.
- [34] J. Xia *et al.*, "Foreign object detection for electric vehicle wireless charging," *Electronics*, vol. 9, no. 5, p. 805, 2020.
- [35] W. Henry, V. Novak, P. Monat, and E. Kallal, "Wireless power system with capacitive proximity sensing," U.S. Patent, 14/875449, Feb. 28, 2017.
- [36] L. Sieber and S. Chopra, "Systems, methods, and apparatus for living object protection in wireless power transfer applications," U.S. Patent, 14/801559, May 29, 2018.
- [37] T. Poguntke, P. Schumann, and K. Ochs, "Radar-based living object protection for inductive charging of electric vehicles using two-dimensional signal processing," *Wirel. Power Transfer*, vol. 4, no. 2, pp. 88–97, Sep. 2017.
- [38] L. Sieber, G. K. Ombach, H. P. Widmer, M. Bittner, B. Dimke, and S. Chopra, "Systems, methods, and apparatus for living object protection having extended functionality in wireless power transfer applications," U.S. Patent, 14/817813, Jul. 3, 2018.
- [39] Q. Wang, J. R. Lee, and M. Huttere, "Methods and apparatus utilizing time division access of multiple radar modules in living object detection for wireless power transfer applications," U.S. Patent, 14/935098, Nov. 24, 2016.
- [40] S. Y. Jeong, E. S. Lee, C. B. Park, K. C. Seo, and C. T. Rim, "Influences of spurious conductors on long distance inductive power transfer systems," in *Proc. IEEE 79th Veh. Technol. Conf.*, Seoul, 2014, pp. 1–5.
- [41] H. Yang, W. Qiu, and Z. Moussaoui, "Wireless charging system with receiver locating circuitry and foreign object detection," U.S. Patent, 15/690121, Aug. 2, 2018.
- [42] B. Shahsavari, W. Huang, S. Kadetotad, V. BabooGowreesunker, and J. Mattingley, "Foreign object detection in wireless charging systems with multiple power receiving devices present on a power transmitting device," U.S. Patent, 15/875127, Mar. 14, 2019.
- [43] S. Behrooz, W. Huang, S. Kadetotad, and B. V. Gowreesunker, "Wireless charging system with image-processing-based foreign object detection," U.S. Patent, 10/236725, Mar. 19, 2019.
- [44] T. Imura, "Simple equivalent circuit model with foreign object on wireless power transfer via magnetic resonant coupling," in *Proc. IEEE Conf. Antenna Meas. Appl.*, Tsukuba, 2017, pp. 367–370.
- [45] A. J. Russel, B. K. Patel, M. P. Pandya, and Z. Moussaoui, "Wireless charging system with object detection," U.S. Patent, 15/804145, Aug. 2, 2018.
- [46] T.-Y. Yang, "Method and apparatus for controlling wireless induction power supply," U.S. Patent, 14/250, 566, May 21, 2019.
- [47] Y.-C. Wang and C.-W. Chiang, "Foreign metal detection by coil impedance for EV wireless charging system," in *Proc. EVS28 Int. Elect. Veh. Symp. Exhib.*, Goyang, Korea, 2015, pp. 3–6.
- [48] W. J. Files and V. X. Bui, "Wireless power system with foreign object detection and method therefor," U.S. Patent, 15/457858, Sep. 13, 2018.
- [49] K. D. Lee and Z. N. Low, "Systems and methods for detecting and identifying a wireless power device," U.S. Patent, 13/464834, Feb. 2, 2016.
- [50] H. Dorairaj, R. Kumar, and S. Ganguly, "Foreign object detection in inductive coupled devices," U.S. Patent, 12/915975, Nov. 5, 2013.
- [51] A. M. Roy *et al.*, "Foreign object detection in wireless energy transfer systems," U.S. Patent, 16/277148, Jun. 13, 2019.
- [52] A. Van Wageningen and A. A. M. Staring, "Wireless inductive power transfer," U.S. Patent, 16/160, 476, Feb. 14, 2019.
- [53] Y. Akuzawa, K. Sakai, T. Ezoe, and Y. Ito, "Resonant type transmission power supply device and resonant type transmission power supply system," U.S. Patent, 15/107330, Jan. 5, 2017.
- [54] S. R. Lafontaine and I. W. Hunter, "Nonlinear system identification for object detection in a wireless power transfer system," U.S. Patent, 14/107025, May 29, 2018.
- [55] H. Nakano, O. Kozakai, S. Komiyama, and K. Fujimaki, "Wireless power transfer device with foreign object detection, system, and method for performing the same," U.S. Patent, 15/649726, Jul. 10, 2018.

- [56] F. Chen, G. Li, and P. Zhao, "Foreign object detection circuit for wireless charger." U.S. Patent, 15/922925, May 30, 2019.
- [57] S. Fukuda, H. Nakano, Y. Murayama, T. Murakami, O. Kozakai, and K. Fujimaki, "A novel metal detector using the quality factor of the secondary coil for wireless power transfer systems," in *Proc. IEEE MTT-S Int. Microw. Workshop Ser. Innov. Wirel. Power Transmiss.: Technol. Syst. Appl.*, Kyoto, 2012, pp. 241–244.
- [58] V. A. Muratov, P. S. Riehl, and W. Plumb, "Robust foreign objects detection," U.S. Patent, 16/228556, Jun. 27, 2019.
- [59] H. Nakano, O. Kozakai, S. Komiyama, and K. Fujimaki, "Wireless power transfer device with foreign object detection, system, and method for performing the same," U.S. Patent, 16/004,930, Oct. 11, 2018.
- [60] S. Huang, J. Su, S. Dai, C. Tai and T. Lee, "Enhancement of wireless power transmission with foreign-object detection considerations," in *Proc. IEEE 6th Glob. Conf. Consum. Electron.*, Nagoya, 2017, pp. 1–2.
- [61] M. Singh and S. Bastami, "Apparatus, system, and method for detecting a foreign object in an inductive wireless power transfer system based on input power," U.S. Patent, 13/436309, Jan. 24, 2017.
- [62] M. Lannoije, J. De Clercq, G. V. Bossche, and J. Martens, "Object detection system and method for operating an object detection system," U.S., 14/901218, Oct. 16, 2018.
- [63] Z. Liu, Q. Zhu, and M. Su, "Metal object detection based on load impedance and input power characteristics for high-dimensional WPT system," *Elect. Eng. Syst. Sci.*, arXiv:1907.0152, Jun. 27, 2019.
- [64] J. Patino, S. N. Thekkevalappil, and S. Sibecas, "Energy transfer optimization by detecting and mitigating magnetic saturation in wireless charging with foreign object detection," U.S. Patent, 10/014,732, Jul. 3, 2018.
- [65] I. Lovas, Z. Mynar, and J. Cicka, "Methods and systems for foreign object detection in wireless energy transfer systems," U.S. Patent, 15/690409, Feb. 28, 2019.
- [66] A. V. Muratov and E. G. Oettinger, "Systems and methods of wireless power transfer with interference detection," U.S. Patent, 13/032, 524, Mar. 22, 2016.
- [67] L. Lan *et al.*, "Foreign object detection for wireless power transfer," in *Proc. 2nd URSI Atlantic Radio Sci. Meeting*, May 20 18, pp. 1–2.
- [68] S. Y. Jeong, V. X. Thai, J. H. Park, and C. T. Rim, "Self-inductance-based metal object detection with mistuned resonant circuits and nullifying induced voltage for wireless EV chargers," *IEEE Trans. Power Electron.*, vol. 34, no. 1, pp. 748–758, Jan. 2019.
- [69] S. Y. Jeong, H. G. Kwak, G. C. Jang, S. Y. Choi, and C. T. Rim, "Dual-purpose nonoverlapping coil sets as metal object and vehicle position detections for wireless stationary EV chargers," *IEEE Trans. Power Electron.*, vol. 33, no. 9, pp. 7387–7397, Sep. 2018.
- [70] A. M. Roy, N. Katz, and N. E. Atnafu, "Foreign object detection in wireless energy transfer systems," U.S. Patent, 16/026,123, Aug. 6, 2019.
- [71] S. Chopra, L. A. Percebon, and M. Werner, "Sense coil geometries with improved sensitivity for metallic object detection in a predetermined space," U.S. Patent, 14/818,051, Nov. 6, 2018.
- [72] L. Percebon and D. Kuerschner, "Hybrid foreign object detection (FOD) loop array board," U.S. Patent, 10/124687, Nov. 13, 2018.
- [73] D. T. Nguyen and C. J. White, "Foreign object detection in a wireless power transfer system," U.S. Patent, 15/416,443, Jul. 26, 2018.
- [74] L. Xiang, Z. Zhu, J. Tian, and Y. Tian, "Foreign object detection in a wireless power transfer system using symmetrical coil sets," *IEEE Access*, vol. 7, pp. 44622–44631, 2019.
- [75] H. Zhang, D. Ma, X. Lai, X. Yang, and H. Tang, "The optimization of auxiliary detection coil for metal object detection in wireless power transfer," in *Proc. IEEE PELS Workshop Emer. Technol.: Wirel. Power Transfer*, Montréal, QC, 2018, pp. 1–6.
- [76] S. Y. Chu and A. Avestruz, "Electromagnetic model-based foreign object detection for wireless power transfer," in *Proc. 20th Workshop Control Model. Power Electron.*, Toronto, ON, Canada, 2019, pp. 1–8.
- [77] U. Omae and T. Kiyakawauchi, "Detection apparatus, power supply system, and method of controlling detection apparatus," U.S. Patent, 14/259,358, Feb. 13, 2018.
- [78] S. Maniktala, "Foreign object detection in wireless power transfer by asymmetry detection," U.S. Patent, 15/967, 912, Nov. 8, 2018.
- [79] K. Maikawa and T. Imazu, "Contactless electricity supply device with foreign object detector," U.S. Patent, 13/822, 260, Jan. 24, 2017.
- [80] B. Zhou, Z. Z. Liu, H. X. Chen, H. Zeng, and T. Hei, "A new metal detection method based on balanced coil for mobile phone wireless charging system," in *Proc. Int. Conf. New Energy Future Energy Syst.*, Aug. 2016, pp. 1–9.
- [81] D. P. Meichle, "Foreign object detection in wireless energy transfer systems," U.S. Patent, 16/111,990, Dec. 20, 2018.
- [82] J. Baek, B. Lee, Y. Cho, and B. Choi, "Foreign object detection apparatus and wireless charging system including the same," U.S. Patent, 16/038,625, Jan. 24, 2019.
- [83] H. Abe, "Contactless power supplying system and metal foreign object detection device of contactless power supplying system," U.S. Patent, 13/806799, Aug. 4, 2015.
- [84] S. Hyodo, "Method for detecting metal foreign object on contactless power supply device, contactless power supply device, contactless power reception device, and contactless power supply system," U.S. Patent, 13/632261, Jan. 5, 2016.
- [85] H. Widmer, "Systems, methods, and apparatus for foreign object detection loop based on inductive thermal sensing," U.S. Patent, 16/414,638, Sep. 5, 2019.
- [86] L. Sieber, M. Fischer, and H. Widmer, "Systems, methods, and apparatus for increased foreign object detection loop array sensitivity," U.S. Patent, 14/218516, Mar. 20, 2018.
- [87] H. P. Widmer, A. Daetwyler, and L. Sieber, "Foreign object detection for ferromagnetic wire-like objects," U.S. Patent, 15/498094, Nov. 1, 2018.
- [88] H. Widmer, M. Bittner, L. Sieber, and M. Fischer, "Systems, methods, and apparatus for detection of metal objects in a predetermined space," U.S. Patent, 13/791,585, Aug. 8, 2017.
- [89] X. Liu, L. H. Swaans, W. K. P. Chan, H. K. Low, and W. K. Chan, "Methods and systems for detecting foreign objects in a wireless charging system," U.S. Patent, 10/305332, May 28, 2019.
- [90] L. Sieber, H. P. Widmer, and A. Daetwyler, "Hybrid foreign-object detection and positioning system," U.S. Patent, 16/052,445, Mar. 21, 2019.
- [91] A. Asano, K. Furiya, J. Araki, and M. Goto, "Power transmission system, foreign object detection device, and coil device," U.S. Patent, 15/543055, Jan. 25, 2018.
- [92] A. Filippenko and M. Kocher, "Method and device for foreign object detection in induction electric charger," U.S. Patent, 14/904,209, Feb. 13, 2018.
- [93] V. X. Thai, J. H. Park, S. Y. Jeong, and C. T. Rim, "Multiple comb pattern-based living object detection with enhanced resolution design for wireless electric vehicle chargers," in *Proc. Int. Exh. Conf. Power Electron. Intell. Motion Renewable Energy Energy Manage.*, Nuremberg, Germany, 2018, pp. 1–6.
- [94] *The Qi Wireless Power Transfer System Power Class 0 Specification: Reference Designs, Wireless Power Consortium*, Feb. 2017, part 4.
- [95] Y. H. Sohn, B. H. Choi, E. S. Lee, G. C. Lim, G. Cho, and C. T. Rim, "General unified analyses of two-capacitor inductive power transfer systems: Equivalence of current-source SS and SP compensations," *IEEE Trans. Power Electron.*, vol. 30, no. 11, pp. 6030–6045, Nov. 2015.
- [96] R. L. Steigerwald, "A comparison of half-bridge resonant converter topologies," *IEEE Trans. Power Electron.*, vol. 3, no. 2, pp. 174–182, Apr. 1988.
- [97] G. Buja, M. Bertoluzzo, and K. N. Mude, "Design and experimentation of WPT charger for electric city car," *IEEE Trans. Ind. Electron.*, vol. 62, no. 12, pp. 7436–7447, Dec. 2015.
- [98] J. Lu, G. Zhu, D. Lin, Y. Zhang, J. Jiang, and C. C. Mi, "Unified load-independent ZPA analysis and design in CC and CV modes of higher order resonant circuits for WPT systems," *IEEE Trans. Transport. Electrific.*, vol. 5, no. 4, pp. 977–987, Dec. 2019.
- [99] *Wireless Power Transfer for Light-Duty Plug-In/Electric Vehicles and Alignment Methodology*. SAE J2954, Nov. 2017.
- [100] S. Y. Jeong, J. H. Park, G. P. Hong, and C. T. Rim, "Autotuning control system by variation of self-inductance for dynamic wireless EV charging with small air gap," *IEEE Trans. Power Electron.*, vol. 34, no. 6, pp. 5165–5174, Jun. 2019.
- [101] G. Buja, M. Bertoluzzo, and H. K. Dashora, "Lumped track layout design for dynamic wireless charging of electric vehicles," *IEEE Trans. Ind. Electron.*, vol. 63, no. 10, pp. 6631–6640, Oct. 2016.
- [102] C. Huang, J. E. James, and G. A. Covic, "Design considerations for variable coupling lumped coil systems," *IEEE Trans. Power Electron.*, vol. 30, no. 2, pp. 680–689, Feb. 2015.
- [103] X. Qu, Y. Jing, H. Han, S. Wong, and C. K. Tse, "Higher order compensation for inductive-power-transfer converters with constant-voltage or constant-current output combating transformer parameter constraints," *IEEE Trans. Power Electron.*, vol. 32, no. 1, pp. 394–405, Jan. 2017.
- [104] F. Liu, K. Chen, Z. Zhao, K. Li, and L. Yuan, "Transmitter-side control of both the CC and CV modes for the wireless EV charging system with the weak communication," *IEEE Trans. Emerg. Sel. Topics Power Electron.*, vol. 6, no. 2, pp. 955–965, Jun. 2018.



Jianghua Lu (Student Member, IEEE) received the M.S. and Ph.D. degrees from the Wuhan University of Technology, Wuhan, China, in 2016 and 2020, respectively.

From September 2018 to October 2020, he was a joint Ph.D. student funded by the China Scholarship Council with the Department of Electrical and Computer Engineering, San Diego State University, San Diego, CA, USA. His research interests include wireless power transfer and resonant converters.



Chunting Chris Mi (Fellow, IEEE) received the B.S.E.E. and M.S.E.E. degrees in electrical engineering from Northwestern Polytechnical University, Xi'an, China, and the Ph.D. degree in electrical engineering from the University of Toronto, Toronto, ON, Canada, in 1985, 1988, and 2001, respectively.

He is a Professor and Chair of Electrical and Computer Engineering and the Director of the Department of Energy (DOE)-funded Graduate Automotive Technology Education (GATE) Center for Electric Drive Transportation, San Diego State University, San Diego, CA, USA. He was with University of Michigan, Dearborn, MI, USA, from 2001 to 2015.



Guorong Zhu (Senior Member, IEEE) received the Ph.D. degree in electrical engineering from the Huazhong University of Science and Technology, Wuhan, China, in 2009.

From 2002 to 2005, she was a Lecturer with the School of Electrical Engineering, Wuhan University of Science and Technology. From 2009 to 2011, she was a Research Assistant/Research Associate with the Department of Electronic and Information Engineering, Hong Kong Polytechnic University, Kowloon, Hong Kong. She is currently an Associate Professor

with the School of Automation, Wuhan University of Technology. Her research interests include wireless power transfer and the reliability of power electronics systems.